Acta Cryst. (1999). B**55**, 953–962

Crystal structure of layered bis(ethylenediamine)nickel hexavanadate as a new representative of the V_6O_{14} series

Peter Y. Zavalij,* Fan Zhang and M. Stanley Whittingham

Materials Research Center, Binghamton University, Vestal Pkwy East, Binghamton, NY 13902-6000, USA. E-mail: zavalij@binghamton.edu

(*Received 13 May 1998; accepted 19 April 1999*)

Abstract

A new $[Ni(NH_2CH_2CH_2NH_2)_2](V_6O_{14})$ compound has been synthesized hydrothermally and was found to crystallize in the monoclinic system. The single-crystal X-ray data leads to a disordered structure, which can be decomposed into two ordered models with different stacking of the V_6O_{14} layers. The structure of the layer is the same in both models and represents a new member of the V_6O_{14} series. All known structures from this series are constructed from the same chain of square pyramids (SP), which share alternatively adjacent or opposite edges of their bases. The differences lie in the orientation of the SP chains which are joined together by sharing corners with tetrahedra to form the layers. Combinatorial analysis of the V_6O_{14} structures was conducted, yielding ten possible symmetry groups for the series of V_6O_{14} layers. The known structures belong only to the three simplest cases with the highest symmetry.

1. Introduction

There has been much interest in the past two decades in layered vanadium oxides and their intercalates because of their potential use as secondary cathode materials for advanced lithium batteries (Whittingham, 1976; Walk & Gore, 1975; Whittingham *et al.*, 1996). Thus, the already rich crystal chemistry of the vanadates with open frameworks has been considerably replenished with many new structures. A significant number of them were determined by our group and include the layered structures $Li_xV_{2-\delta}O_{4-\delta}$ (Chirayil *et al.*, 1996*a*), $Li_xV_{2-\delta}O_{4-\delta}.H_2O$ (Chirayil *et al.*, 1996*b*), $(tma)_8V_3O_7$ {tma = tetramethylammonium, $[N(CH_3)_4]^+$} (Zavalij *et al.*, 1997*a*), $(tma)_8V_4O_{10}$ (Zavalij *et al.*, 1996), $(ma)V_3O_7$, $(ma)V_4O_{10}$ [ma = methylammonium, $(CH_3NH_3)^+$; Chen, Zavalij & Whittingham, 1999] and $(tma)V_8O_{20}$ (Chirayil, Zavalij & Whittingham, 1997), the three-dimensional framework structures $Zn_3(OH)_2(V_2O_7).2H_2O$ (Zavalij, Zhang & Whittingham, 1997), $Zn_2(OH)_3(VO)_3$ (Zhang *et al.*, 1998) and $Al_2(OH)_3(VO_4)$ (Pecquenard *et al.*, 1998*a*), the chain structures $VO(OCH_2CH_2O)$ and $VO(CH_3COO)_2$ (Weeks *et al.*, 1999), and also the clusters $[Li(H_2O)]_2(tma)_4(V_{10}O_{28}).4H_2O$ (Zavalij, Whittingham *et al.*, 1997), $Na_4(tma)_2(V_{10}O_{28})].20H_2O$ (Zavalij *et al.*, 1997*b*), $[CH_3(CH_2)_{11}N(CH_3)_3]_4(H_2V_{10}O_{28}).8H_2O$ (Janauer *et al.*, 1997), $(tma)_4(H_2V_{10}O_{28}).CH_3COOH.2.7H_2O$ (Pecquenard *et al.*, 1998*b*) and $(tma)_8[(CH_3COO)V_{22}O_{54}].4.25H_2O$ (Chirayil *et al.*, 1998).

Such great interest in vanadium compounds arises from the variety of oxidation states of vanadium and the redox properties of such compounds, which readily allow the insertion/removal of ions such as lithium. The structure of these frameworks is defined in substantial part by the vanadium coordination polyhedra: for instance, a rectilineal octahedron for V(+3) and a tetrahedron (T) for V(+5) in its classic compounds such as orthovanadates, metavanadates, *etc*. Most interest has centered on compounds with oxidation states between +3 and +5 with square pyramidal (SP) and distorted octahedral coordination polyhedra. They are similar to one another and generally contain double-bonded oxygen (VO vanadyl group) in the vertex; the octahedron has an additional weakly bonded oxygen in the apex opposite to the vanadyl group. This makes it possible to change the oxidation state of vanadium without significant deformation of the framework.

It was shown earlier (Chirayil, Boylan *et al.*, 1997) that using mild hydrothermal synthesis it is possible to control framework (polyhedra) type simply by changing the pH. Basic media (pH > 8) obviously lead to the classic tetrahedral structures. The lowest pH (< 3.5) results in frameworks built from distorted octahedra, but a moderate acidic medium (pH 3.5–5) produces layers of square pyramids. The region between weak acid and weak base (pH 5.5–8) combines both square pyramids and tetrahedra; this type of vanadium oxide layer, built by corner-sharing square pyramids or pairs of square pyramids and tetrahedra, was found in compounds such as $K_2V_3O_8$ (Galy & Carpy, 1975), $Cs_2V_5O_{13}$ (Waltersson & Forslund, 1977*a*), $K_3V_5O_{14}$ (Evans & Brusewitz, 1994), CsV_2O_5 (Waltersson & Forslund, 1977*b*), and $(LH_2)(V_2O_5)_2$, where *L* is 1,3-diaminopropane (Riou & Férey, 1995*a*), ethylenediamine or piperazine (Riou & Férey, 1995*b*).

© 1999 International Union of Crystallography
Printed in Great Britain – all rights reserved

ISSN 0108-7681 © 1999

Table 1. *Experimental details*

Crystal data		
Chemical formula	$[Ni(C_2H_8N_2)_2](V_6O_{14})$	
Model	Disordered	Ordered
Chemical formula weight	708.59	708.59
Cell setting	Monoclinic	Monoclinic
Space group	$P2_1/c$	$P2_1/n$
a (Å)	8.9311 (11)	17.862 (2)
b (Å)	17.127 (2)	17.127 (2)
c (Å)	6.6270 (8)	6.6270 (8)
β (°)	111.610 (2)	111.610 (2)
V (Å^3)	942.4 (3)	1884.9 (7)
Z	2	4
$F(000)$ (Mg m^{-3})	692	1384
D_x (Mg m^{-3})	2.497	2.497
Radiation type	Mo $K\alpha$	
Wavelength (Å)	0.71073	
No. of reflections for cell parameters	1430	
θ range (°)	4.7–28	
μ (mm^{-1})	3.90	
Temperature (K)	295	
Crystal form	Plate	
Crystal size (mm)	0.41 × 0.16 × 0.06	
Crystal color	Black	
Data collection		
Diffractometer	Siemens Smart CCD	
Data collection method	Frame scans	
Absorption correction	Multi-scan *SADABS* (Sheldrick, 1996)	
T_{min}	0.641	
T_{max}	0.777	
No. of measured reflections	3679	
No. of independent reflections	1684	
No. of observed reflections	1267	
Criterion for observed reflections	$F_o > 4\sigma(F_o)$	
R_{sig}	0.0508	
R_{int}	0.0514	
θ_{max} (°)	28	
Range of h, k, l	$-8 \rightarrow h \rightarrow 2$ $-11 \rightarrow k \rightarrow 4$ $-21 \rightarrow l \rightarrow 20$	
Intensity decay (%)	0	
Refinement		
Refinement on	F	
R	0.0600	
wR	0.0637	
S	1.29	
No. of reflections used in refinement	1267	
No. of parameters used	165	
H-atom treatment	H-atom parameters not refined	
Weighting scheme	$w = 1/[\sigma^2(F_o) + 0.002F_o^2)]$	
$(\Delta/\sigma)_{max}$	0.01	
$\Delta\rho_{max}$ (e Å^{-3})	0.93	
$\Delta\rho_{min}$ (e Å^{-3})	−1.22	
Extinction correction	None	
Source of atomic scattering factors	*International Tables for X-ray Crystallography* (1974, Vol. IV)	

Table 1 (*cont.*)

Computer programs	
Data collection	*SMART* (Siemens, 1995)
Cell refinement	*SAINT* (Siemens, 1995)
Data reduction	*SAINT*
Structure solution	*CSD* (Akeslrud *et al.*, 1989)
Structure refinement	*CSD*
Molecular graphics	*ORTEP*III (Farrugia, 1997), *Crystal-Designer* (Crystal Structure Design, 1997), *Insight*II (Biosym Technologies Inc., 1995)

In the past few years, compounds have been synthesized with a new type of SP–T layer built from continuous chains of square pyramids linked together by tetrahedra. The distinguishable peculiarity of this type of layer is chains of edge-shared square pyramids that cause strong interaction between V atoms; therefore, such compounds are more attractive for electrochemical use because of their ability to delocalize and distribute the charge density. These compounds were prepared hydrothermally: (dabco)V_6O_{14} {dabco = $[HN(CH_2CH_2)_3NH]^{2+}$} by Nazar *et al.* (1996) and Zhang, Haushalter & Clearfield (1996), $(eda)_2M^{2+}V_6O_{14}$ [eda = ethylenediamine, $NH_2(CH_2)_2NH_2$, $M^{2+} = Cu^{2+}$, Zn^{2+}] by Zhang, DeBord *et al.* (1996), (tma)V_3O_7 by Zavalij *et al.* (1997*a*), and (ma)V_3O_7 by Chen *et al.* (1999). All four of these layers appear different, even though they are built by identical chains of square pyramids joined by tetrahedra sharing two corners with one chain, and a third corner with a second chain.

This work presents the crystal structure of $(eda)_2NiV_6O_{14}$, a new fifth member of this series, and a combinatorial analysis of V_6O_{14} layers, which allows the derivation of all possible types of these layers. The order–disorder nature of the title structure is also discussed.

2. Experimental

The title compound was prepared by the hydrothermal treatment of V_2O_5, $NiSO_4$ and $NH_2(CH_2)_2NH_2$ (eda) in a 1:1:4 molar ratio. The reaction mixture was heated in a 125 ml Teflon-lined Parr reactor for 2.5 d at 438 K. Two types of compounds co-crystallize: black plate crystals and light-violet needle crystals. The crystal structure of the black $(eda)_2NiV_6O_{14}$ crystals was solved by direct methods using *CSD* software (Akselrud *et al.*, 1989) from single-crystal data collected on a Siemens CCD diffractometer at Syracuse University. Experimental details are given in Table 1. The $(eda)_2NiV_6O_{14}$ structure was found to be disordered; therefore, its treatment was not routine. The knowledge of similar structures was applied to resolve two overlapped layers, considering two possible ways of stacking the layers, as described in the following section. The second violet phase was identified as tris(ethylenediamine)nickel(II) sulfate,

$(eda)_3NiSO_4$, with known structure (Mazhar-Ul-Haque *et al.*, 1970).

3. Crystal structure of $(eda)_2NiV_6O_{14}$

Bis(ethylenediamine)nickel(II) hexavanadate crystallizes in a monoclinic lattice; its structure was solved in space group $P2_1/c$. An ordered structure was obtained initially and refined in isotropic approximation to R = 0.15 and then in anisotropic approximation to R = 0.07. Such a rapid decrease in R factor was caused by the enormous anisotropy of certain atoms (Fig. 1*a*). However, the structural model, polyhedra and geometric parameters made sense. The structure was built up from $(eda)_2Ni$ complexes that link V_6O_{14} layers into a three-dimensional framework, similar to other $(eda)_2MV_6O_{14}$ (M = Zn, Cu) compounds (Zhang, DeBord *et al.*, 1996). The difference lies in the structure of the layer, consisting of corner-shared square pyramids and slightly distorted tetrahedra (Fig. 2*a*) in the case of the Ni compound, whereas in the Zn and Cu compounds edge-sharing square pyramids form chains that are linked into the layer by sharing corners with tetrahedra. Nevertheless, as became clear later, this model was not correct. The significant peaks on the difference Fourier map that were close (0.3–0.7 Å) to already included atoms still remained even after anisotropic refinement was carried out. The refinement of the disordered model led to a lower R factor, but six of the 15 non-H atoms split into two, with occupation factors of around 0.5 (Fig. 1*b*). The final refinement of the disordered model used an isotropic (split atoms) and anisotropic (non-split atoms) approximation (Table 2). H atoms of the eda molecule were partly found from difference Fourier synthesis and partly calculated from geometrical considerations, and were not included in the refinement. It has to be emphasized that in the case of this disordered model, anisotropic displacement parameters for non-split atoms do not quite fit the definition of the term. In fact all atoms are split, but for so-called 'non-split' atoms this splitting is not distinguishable from the experimental data used. Therefore, anisotropic displacement parameters for those atoms, differing in their split positions by less than 0.3 Å, include their real thermal motion parameters, and, as usual, other negligible corrections.

The disorder in the nickel vanadate structure is so significant that it should not be left without further analysis. Not all atoms split (here and in further discussion the atoms will be called 'split' when they split by more than 0.3 Å). One vanadium atom (V1), three oxygen atoms (O1, O2, O3) and all atoms of the $(eda)_2Ni$ complex are considered as not split according to the aforementioned definition. The remaining V and O atoms split into pairs: V2—V4 0.457 (5), V3—V5 0.435 (5), O4—O8 0.36 (2), O5—O9 0.37 (2), O6—O10 0.61 (2), O7—O11 0.73 (2) Å.

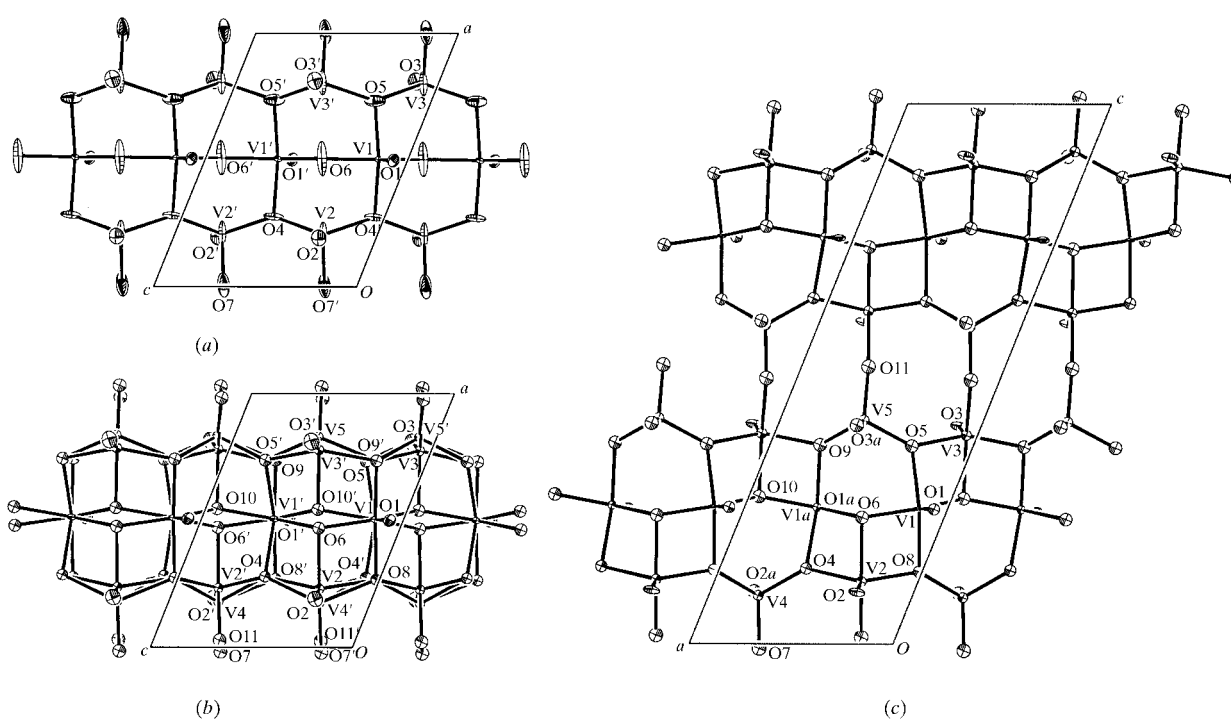

Fig. 1. Displacement ellipsoids shown at 50% probability for the V_6O_{14} layer of $(eda)_2NiV_6O_{14}$: (*a*) 'anisotropic' model; (*b*) disordered model; (*c*) ordered model.

This model suggests two different orientations or positions of the vanadium oxide layer, which overlap in the average diffraction picture. Analysis of the coordination polyhedra of the split V atoms, employing basic knowledge about the crystal chemistry of vanadium oxide structures (possible coordination polyhedra) and knowledge about the structure of the V_6O_{14} vanadium oxide layers, allowed the recovery of an ordered model of the layer from the overlapped 'disordered' structure. For instance, the split V2—V4 and V3—V5 pairs can be considered as atoms with different coordination: square pyramidal for V2 and V3, and tetrahedral for V4 and V5. The next step is to find the ordered distribution of these square pyramids and tetrahedra. There are a few different distributions, of which only one makes chemical sense; its analogue is present among known vanadium oxide layers. This ordered model of the layer, shown in Fig. 2(*b*), can be built only in the absence of the *c* glide plane. Moreover, it is necessary to double the *a* parameter of the cell to reach an agreement in stacking the chains and in turn an *n* glide plane appears. Thus,

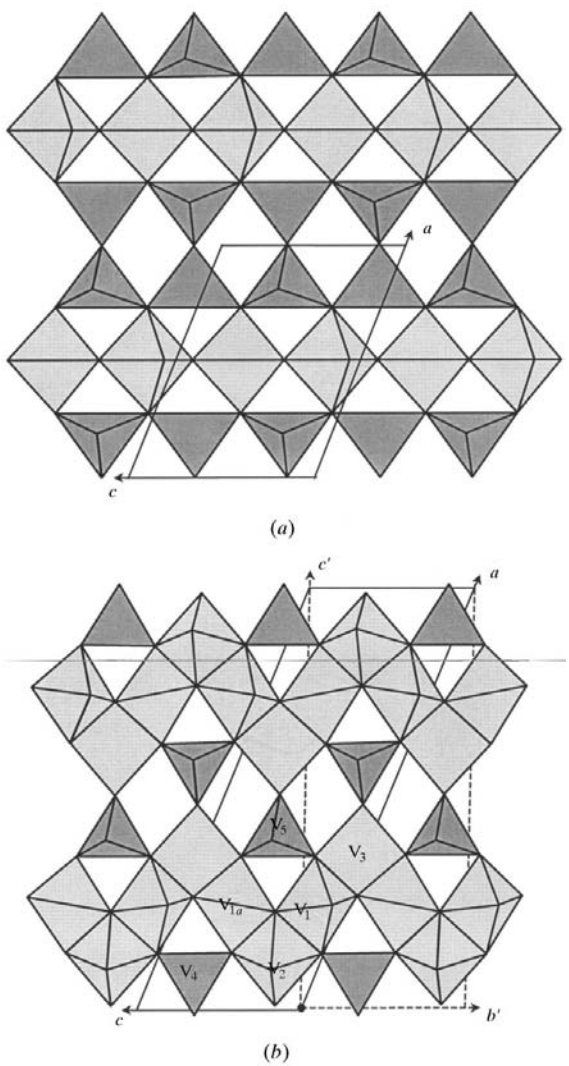

Fig. 2. Polyhedral representation of the V_6O_{14} layer in (*a*) the incorrect 'anisotropic' model and (*b*) the ordered model. In the latter, *c'* and *b'* axes refer to the setting used in Table 5.

Table 2. *Fractional atomic coordinates and equivalent isotropic displacement parameters (Å²)*

$$U_{eq} = (1/3)\Sigma_i\Sigma_j U^{ij} a^i a^j \mathbf{a}_i.\mathbf{a}_j.$$

	Occupation	*x*	*y*	*z*	U_{eq}
Disordered model					
V1		0.50362 (1)	0.20999 (7)	0.1424 (2)	0.0079 (5)
V2	0.5	0.2310 (3)	0.2133 (2)	0.2810 (5)	0.0099 (4)
V3	0.5	0.7774 (3)	0.2894 (2)	0.0584 (5)	0.0107 (4)
V4	0.5	0.1761 (3)	0.2878 (2)	0.7532 (5)	0.0099 (4)
V5	0.5	0.8294 (3)	0.2133 (2)	0.5882 (5)	0.0107 (4)
O1		0.5012 (6)	0.1194 (3)	0.0690 (8)	0.017 (2)
O2		0.1915 (7)	0.1213 (3)	0.2816 (9)	0.023 (2)
O3		0.8104 (7)	0.3796 (3)	0.1123 (9)	0.025 (2)
O4	0.5	0.277 (2)	0.2578 (8)	0.574 (2)	0.013 (2)
O5	0.5	0.735 (2)	0.2399 (8)	0.303 (2)	0.017 (2)
O6	0.5	0.4683 (14)	0.2191 (7)	0.404 (2)	0.016 (2)
O7	0.5	−0.0196 (14)	0.2669 (7)	0.644 (2)	0.019 (2)
O8	0.5	0.269 (2)	0.2373 (8)	0.018 (2)	0.013 (2)
O9	0.5	0.736 (2)	0.2686 (8)	0.752 (2)	0.017 (2)
O10	0.5	0.5417 (14)	0.2807 (7)	−0.055 (2)	0.016 (2)
O11	0.5	1.0262 (14)	0.2304 (7)	0.671 (2)	0.019 (2)
Ni		1/2	1/2	1/2	0.0125 (6)
C1		0.1524 (10)	0.5164 (6)	0.3504 (14)	0.028 (4)
C2		0.1855 (11)	0.4566 (6)	0.201 (2)	0.033 (4)
N1		0.2871 (9)	0.5160 (4)	0.5629 (11)	0.025 (3)
N2		0.3419 (8)	0.4757 (4)	0.1903 (10)	0.021 (3)
Ordered model II					
Ni1		1/2	1/2	1/2	0.0098 (4)
Ni1*a*		1/2	0	1	0.0098 (4)
V1		0.50181 (7)	0.20999 (7)	0.1424 (2)	0.0071 (4)
V2		0.3655 (2)	0.2133 (2)	0.2810 (5)	0.0099 (4)
V3		0.6387 (2)	0.2894 (2)	0.0584 (5)	0.0107 (4)
V4		0.3380 (2)	0.2878 (2)	0.7532 (5)	0.0099 (4)
V5		0.6647 (2)	0.2133 (2)	0.5882 (5)	0.0107 (4)
V1*a*		0.50181 (7)	0.29001 (7)	0.6424 (2)	0.0071 (4)
O1		0.5006 (3)	0.1194 (3)	0.0690 (8)	0.013 (2)
O2		0.3457 (3)	0.1213 (3)	0.2816 (9)	0.017 (2)
O3		0.6552 (4)	0.3796 (3)	0.1123 (9)	0.018 (2)
O4		0.3884 (9)	0.2578 (8)	0.574 (2)	0.013 (2)
O5		0.6177 (9)	0.2399 (8)	0.303 (2)	0.017 (2)
O6		0.4842 (7)	0.2191 (7)	0.404 (2)	0.016 (2)
O7		0.2402 (7)	0.2669 (7)	0.644 (2)	0.019 (2)
O8		0.3843 (9)	0.2373 (8)	0.018 (2)	0.013 (2)
O9		0.6181 (9)	0.2686 (8)	0.752 (2)	0.017 (2)
O10		0.5208 (7)	0.2807 (7)	−0.055 (2)	0.016 (2)
O11		0.7631 (7)	0.2305 (7)	0.671 (2)	0.019 (2)
O1*a*		0.5006 (3)	0.3806 (3)	0.5690 (8)	0.013 (2)
O2*a*		0.3457 (3)	0.3787 (3)	0.7816 (9)	0.017 (2)
O3*a*		0.6552 (4)	0.1204 (3)	0.6123 (9)	0.018 (2)
N1		0.3935 (4)	0.5160 (4)	0.5629 (11)	0.020 (2)
N2		0.4210 (4)	0.4757 (4)	0.1903 (10)	0.017 (2)
N1*a*		0.3935 (4)	−0.0160 (4)	1.0629 (11)	0.020 (2)
N2*a*		0.4210 (4)	0.0243 (4)	0.6903 (10)	0.017 (2)
C1		0.3262 (5)	0.5164 (6)	0.3504 (14)	0.026 (3)
C2		0.3428 (6)	0.4566 (6)	0.201 (2)	0.029 (3)
C1*a*		0.3262 (5)	−0.0164 (6)	0.8504 (14)	0.026 (3)
C2*a*		0.3428 (6)	0.0434 (6)	0.701 (2)	0.029 (3)

space group $P2_1/c$ is converted into $P2_1/n$ with a doubled a parameter. The coordinates of the split atoms in the disordered model were transformed by symmetry operations in a way that made it easier to convert atoms into the ordered model: the atoms have to be simply copied with $x_o = x_d/2$ (where o refers to ordered and d disordered structures). There is a single obvious feature that the 'non-split' atoms [V1, O1, O2, O3 and the atoms of the $(eda)_2Ni$ complex] have to be copied twice: themselves and their image transformed by the c glide plane. Thus, there are the following transformations

$$\mathbf{a}_o = 2\mathbf{a}_d$$
$$\mathbf{b}_o = 2\mathbf{b}_d$$
$$\mathbf{c}_o = 2\mathbf{c}_d$$

for the unit cell;

$$x_o = x_d/2$$
$$y_o = y_d$$
$$z_o = z_d$$

for all atoms; and additionally

$$x_o = x_d/2$$
$$y_o = 1/2 - y_d$$
$$z_o = 1/2 + z_d$$

for the 'non-split' atoms excluding nickel. These additional atoms are marked with the letter a after the numerical part of the atom identifier in Fig. 1(c), where the ball-and-stick model of the ordered V_6O_{14} layer is presented. The polyhedral representation is depicted in Fig. 2(b). Two types of square pyramid form zigzag chains along the c axis: the so-called 'middle' SP (V1, V1a) shares opposite edges of the base, whereas the 'corner' SP (V2, V3) shares neighboring edges. The tetrahedron (V4, V5), which shares two corners with one chain and one corner with another, links these chains into the layer. This zigzag SP chain with two rows of T on both sides will be called the 'SPT chain', and the layers it forms the 'SPT layers'.

It appears that two different ordered models with the same space group, $P2_1/n$, can be derived from the disordered structure (space group $P2_1/c$). The first model (I) is described above and the second model (II) can be obtained from model I simply by a 0.25 shift along the x axis applied to all atoms in the asymmetric unit, or from the disordered model by the following transformation

$$x_o = x_d/2 + 1/4$$
$$y_o = y_d$$
$$z_o = z_d$$

for all atoms; and additionally

$$x_o = x_d/2 + 1/4$$
$$y_o = 1/2 - y_d$$
$$z_o = 1/2 + z_d$$

for the 'non-split' atoms including nickel. The difference between these two models is shown in Fig. 3, where the layers at $y = 1/4$ coincide and at $y = 3/4$ are different. Two apical O atoms from the middle SP coordinate the Ni atom that forms a bridge between the layers. The V_6O_{14}

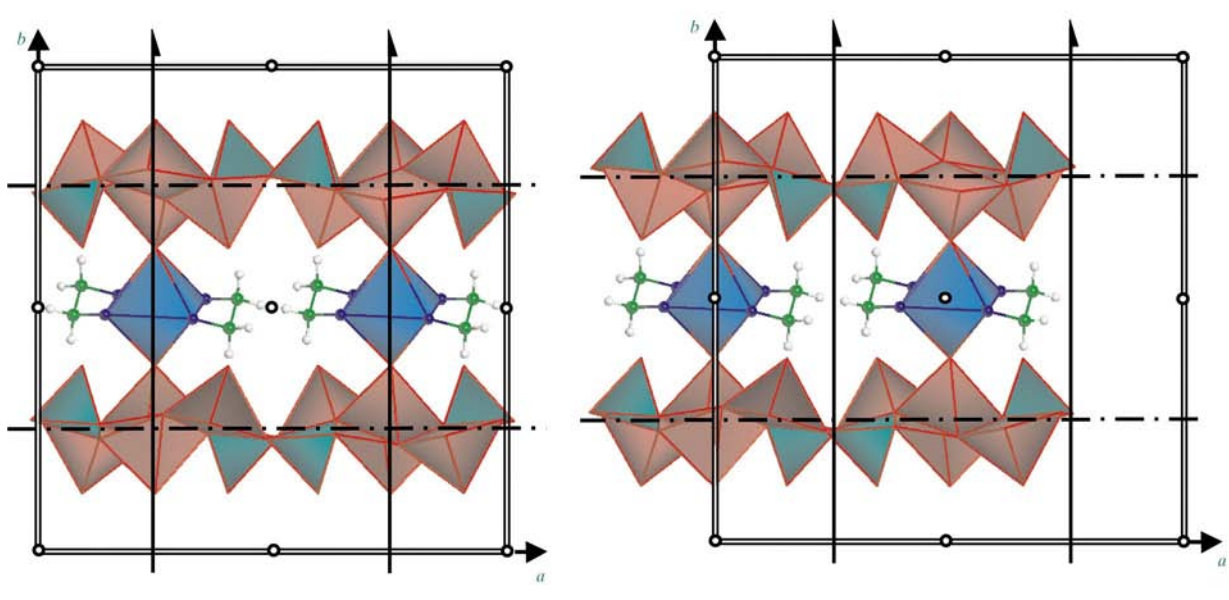

(*a*) (*b*)

Fig. 3. Stacking of the layers in (*a*) model I and (*b*) model II.

layers are identical in both models, but pairs of layers are different. This difference is significant from a crystallographic point of view. Thus, in model I a pair of SPT chains linked by the same Ni atom are transformed into

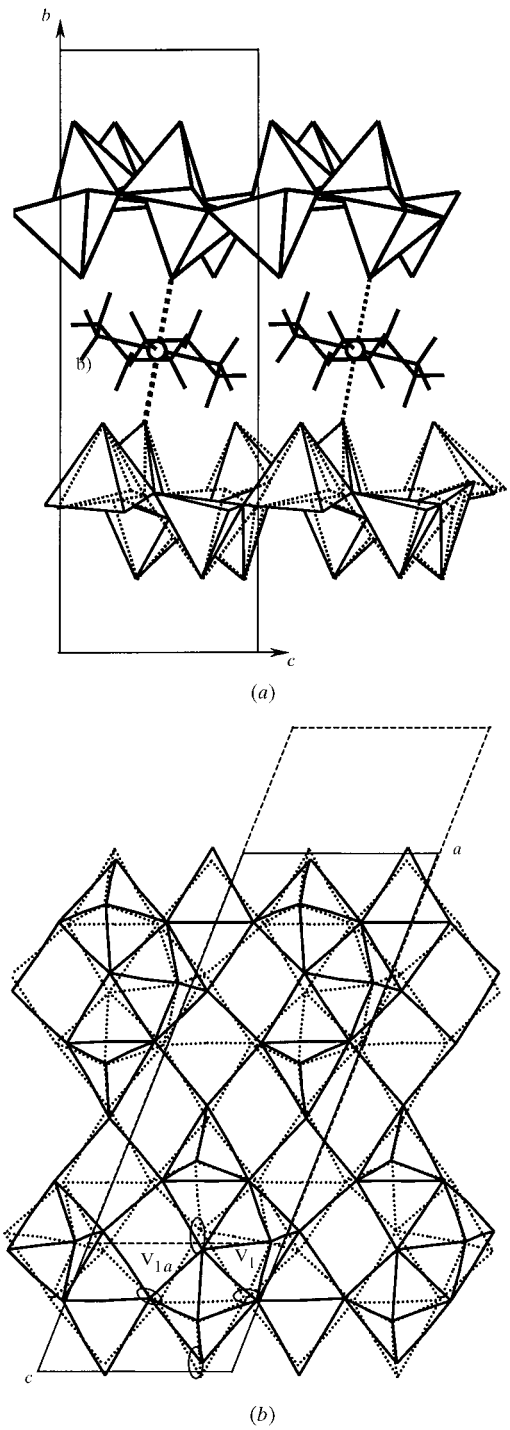

Fig. 4. Order–disorder (*a*) in two different pairs of V_6O_{14} layers overlapped in a view along the *a* axis, and (*b*) superposition of two layers. Solid and dotted lines represent models I and II, respectively.

Table 3. *Selected geometric parameters (Å, °) for ordered model II*

Ni1—N2	2.060 (6)	V3—O5	1.981 (14)
Ni1—O1*a*	2.095 (5)	V4—O2*a*	1.569 (6)
Ni1—N1	2.109 (8)	V4—O7	1.666 (14)
Ni1*a*—N2*a*	2.060 (6)	V4—O4	1.809 (15)
Ni1*a*—O1^{i}	2.095 (5)	V4—O8^{i}	1.857 (13)
Ni1*a*—N1*a*	2.109 (8)	V5—O3*a*	1.614 (6)
V1—O1	1.624 (5)	V5—O11	1.663 (14)
V1—O6	1.876 (13)	V5—O5	1.823 (13)
V1—O10	1.900 (13)	V5—O9	1.853 (15)
V1—O8	2.01 (2)	V1*a*—O1*a*	1.624 (5)
V1—O5	2.01 (2)	V1*a*—O10^{i}	1.916 (12)
V2—O2	1.617 (6)	V1*a*—O6	1.927 (12)
V2—O8	1.934 (14)	V1*a*—O9	1.97 (2)
V2—O11^{ii}	1.955 (14)	V1*a*—O4	1.98 (2)
V2—O6	1.973 (14)	N1—C1	1.477 (11)
V2—O4	1.983 (13)	N2—C2	1.461 (14)
V3—O3	1.590 (6)	N1*a*—C1*a*	1.477 (11)
V3—O7^{iii}	1.944 (14)	N2*a*—C2*a*	1.461 (14)
V3—O9^{iv}	1.958 (13)	C1—C2	1.527 (15)
V3—O10	1.963 (14)	C1*a*—C2*a*	1.527 (15)

Symmetry codes: (i) $x, y, 1+z$; (ii) $x-\frac{1}{2}, \frac{1}{2}-y, z-\frac{1}{2}$; (iii) $\frac{1}{2}+x, \frac{1}{2}-y, z-\frac{1}{2}$; (iv) $x, y, z-1$.

each other by a 2_1 screw axis (Fig. 3*b*), whereas in model II such a transformation is performed by the $\bar{1}$ inversion center located at the Ni atom (Fig. 3*a*). Therefore, only one Ni atom, in a general position, is present in model I, but there are two independent Ni atoms at centers of symmetry in model II (Table 2). However, no difference between these models in the first coordination sphere for all atoms including hydrogen can be found. As can be seen from Fig. 4(*a*), the Ni atoms, eda atoms, apical O atoms and V1 atom from the middle SP coincide for both models and the rest of the atoms of the V_6O_{14} layer are split. Thus, the corner SP overlaps with tetrahedra and the middle SP (V1) is tilted around the vanadyl bond, as can be seen in Fig. 3(*b*). However, all apical atoms of these polyhedra are located in the same position and form an identical surface for both orientations of the layer. All interatomic distances and angles (Table 3), including hydrogen bonds (Table 4), are essentially the same for both models and therefore are provided only for model II.

The same environment for all atoms, including H atoms, means the same short-range (strong) bonding and, therefore, very close energy for both types of the layer stacking. Thus, the presence of the two pairs of layers is obvious and their alternation causes disorder of the average diffraction structure. According to the classification given by Dornberger-Schiff (1966), the layered structure in which two different pairs of layers are present is an order–disorder structure only when no structure can be built from a single pair of layers. However, in our case the structure can be constructed from any of these pairs (model I and II) and therefore it is not order–disorder. This conclusion was confirmed by electron diffraction, which showed no diffuse or super-

Table 4. *Hydrogen-bonding geometry (Å, °) for ordered model II*

D—H···A	D—H	H···A	D···A	D—H···A
N1—H5···O2*a*	0.96	2.101	3.044	166.99
N1—H6···O3^{i}	0.949	2.366	3.157	140.59
N2—H7···O3^{ii}	0.956	2.28	3.163	153.16
N2—H8···O2*a*^{iii}	0.958	2.491	3.036	116.01
N1*a*—H5*a*···O2^{iv}	0.96	2.101	3.044	166.99
N1*a*—H6*a*···O3*a*^{v}	0.949	2.366	3.157	140.59
N2*a*—H7*a*···O3*a*^{vi}	0.956	2.28	3.163	153.16
N2*a*—H8*a*···O2	0.958	2.491	3.036	116.01

Symmetry codes: (i) $1-x, 1-y, 1-z$; (ii) $1-x, 1-y, -z$; (iii) $x, y, z-1$; (iv) $x, y, 1+z$; (v) $1-x, -y, 2-z$; (vi) $1-x, -y, 1-z$.

lattice reflections. Therefore, the observed disorder is probably due to twinning. On the other hand, all attempts to find a single crystal were not successful and different sets of diffraction experiments yielded the same disordered model, which suggests the presence of the microtwinning effect.

4. Combinatorial deduction of the V_6O_{14} layers

As discussed above, the recently discovered V_6O_{14} layer type is built from VO_5 square pyramids (SP) and VO_4 tetrahedra (T). The square pyramids share opposite (middle SP) or neighboring (corner SP) basal edges to form a zigzag chain. This SP chain, together with T which shares two corners with the chain, is called an SPT chain. This SPT chain is the basic building block for the V_6O_{14} layered structures including the title compound (Table 5). The peculiarity of the zigzag SPT chain is that the bases of the SP together with one of the T faces are more or less coplanar. The apices of SP and T (the last one is defined as the vertex opposite the T face coplanar to the chain) are directed up and down. The middle and corner SP form pairs with apices on one side. The next pair points in the opposite direction. The orientation of T is always opposite most of the adjacent SP (three of four). Therefore, all T on one side of the chain are always pointing in the same direction, whereas all T on the other side are directed oppositely. Thus, only a 2_1 screw axis is present in an ideal SPT chain. The coordinate system used in the further discussion is shown in Fig. 5, where **b** is directed along the chain, **a** is perpendicular to the layer and **c** is perpendicular to the chain and parallel to the layer.

The V_6O_{14} layers are formed by sharing corners of the SP and T from adjacent SPT chains. The chains can have four different orientations, denoted *A*, *B*, *C* and *D* in Fig. 5. Therefore, the SPT chains can join in four different ways: α (*AA*, *BB*, *CC*, *DD*), β (*AB*, *CD*), γ (*AC*, *BD*) and δ (*AD*, *BC*). The symmetry operations that transform one chain into another are as follows: translation in α, inversion center in β, reflection (glide plane) in γ and rotation (2_x) in δ. The β and γ operations give an inverted (enantiomorphous) image of the chain, whereas α and δ simply change the orientation of the chain. The γ and δ operations switch left and right sides (the T between chains point in the same direction), but α and β retain left and right sides of the chains (the T between chains point in opposite directions).

Both the absolute orientation symbols (*ABCD*) and the relative orientation symbols ($\alpha\beta\gamma\delta$) can be used to describe or construct the layers by giving the SPT chain sequence. For example, *ABCD* in absolute symbols is $\beta\delta\beta\delta$ in relative symbols. Obviously, there is an infinite number of possible SPT layers. The known V_6O_{14} structures have α (*AA*) or β (*AB*) types of layers. The title compound is a new member of this family of V_6O_{14} layers and can be described as consisting of *AC* or γ layers. The structure with the δ layer still remains unknown. The four cases, α, β, γ and δ layers, are the simplest in this series and contain chains in one (α or *AA*) or two (*AB*, *AC*, *AD*) orientations. However, only

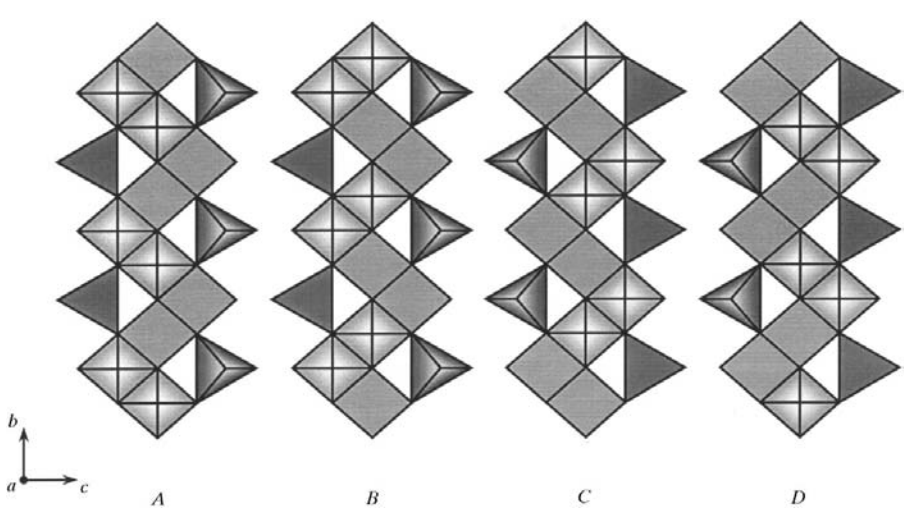

Fig. 5. Four possible relative orientations of the SPT vanadium oxide chains.

Table 5. *The simplest V_6O_{14} layers*

Absolute symbol	Relative symbol	Layer symmetry	Layer dimensions		Interlayer spacing	Representative	Reference
			b (Å)	c (Å)	$a \sin\beta$ (Å)		
A	α	$P12_11$	6.55	8.43	9.24	$(tma)V_3O_7$	Zavalij *et al.* (1997*a*)
AB	β	$P12_1/c1$	6.53	8.37 × 2	8.33	$(eda_2Zn)V_6O_{14}$	Zhang, DeBord *et al.* (1996)†
			6.56	8.33 × 2	8.29	$(eda_2Cu)V_6O_{14}$	
AC	γ	$Pc2_1b$‡	6.63	8.30 × 2	8.56	$(eda_2Ni)V_6O_{14}$	This work§
AD	δ	$P22_12_1$				Unknown	
A'	α'	$P12_11$	6.63	7.55	8.94	$(dabco)V_6O_{14}.H_2O$	Nazar *et al.* (1996),
		6.66		7.57	8.99		Zhang, Haushalter & Clearfield (1996)
$A'B'$	β'	$P12_1/c1$	6.66	7.58 × 2	7.90	$(CH_3NH_3)V_3O_7$	Chen *et al.* (1999)

† Transformed from the originally published coordinate system to the system used in this table as $a' = -a$, $b' = b$, $c' = a + c$. ‡ The layer in the title structure is deformed ($\alpha = 90.17°$) and therefore its symmetry is $Pc11$. § Transformed from the original $P12_1/n1$ to the $P2_1/c11$ setting as $a' = b$, $b' = -c$, $c' = a + c$.

one symmetrically independent chain is present among them, or, in other words, one type of pair α, β, γ or δ (Table 5).

Since two corners of the T are shared within the SPT chain, either one of the two remaining corners can be shared with the SP from the linked chain. Thus, two-way links T–SP and SP–T join the chains into the layer. When the corner of the base of the tetrahedron is shared, flat layers are formed (α, β, γ and δ in Fig. 6). However, the apex of the tetrahedron may also be shared; this sharing leads to the step-like configuration of the layer, which is marked by an apostrophe and shown as α' and β' in Fig. 6. This apical sharing is possible only in the α and β cases, where opposite orientations of the T between the chains occur. The α' and β' joining makes no changes in the symmetry of pairs and, therefore, makes no difference in the symmetry of the layers, but substantially changes the dimensions of the layer (Table 5). In the case of γ and δ pairs, two-way sharing of the apical corners cannot be accomplished because the rows of T on both sides of the join point in the same direction.

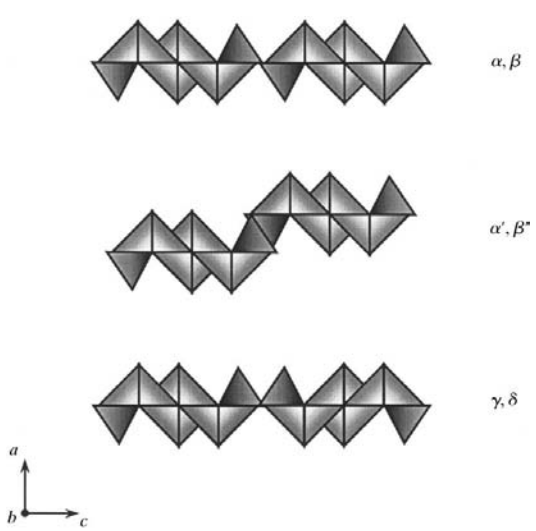

Fig. 6. Two types of linking of the SPT chains in the layers.

Thus, only one of the six possible simplest structures of the V_6O_{14} layers has not been found yet. The symmetry of this δ layer is $p22_12_1$. Therefore, the possible space groups for the structure with the δ layer are $P22_12_1$, *Pnaa*, *Pban*, *Pcna* or *Pmnn* if there is no deformation of the layer. There is only one chain per unit cell along the c axis in the case of α and α' layers, but two chains are required for β, γ and δ stacking. In the last case the c parameters are given in Table 5 as values of $c/2$ marked with '×2' to make them comparable. These values are noticeably different (~0.8 Å) for chains stacking into the flat or step-like layers (Fig. 6). The b parameters of the layer should be equal, but they are 0.1 Å shorter for the first three structures with α and β layers which are twisted more than in the other cases. The variability of the third parameter, the interlayer spacing d, is not obvious at all. For instance, the Zn—O distance of 2.45 Å and Cu—O of 2.52 Å are much greater than Ni—O of 2.09 Å, but the interlayer spacing has the opposite dependence, which is caused by a different tilt of the O—M—O axis relative to the layer. Thus, in the nickel structure this axis is almost perpendicular to the layers, whereas in the Zn and Cu structures the tilt is about 33°.

Using the relative symbols of the V_6O_{14} layers, the combinatorial deduction of their possible symmetry has been conducted and is summarized in Table 6. The repeat unit in the absolute formula is always the same as the repeat unit in the structure of the layer (c dimension), whereas the relative formula unit in some cases is half the size. However, recovering symmetry from the relative symbol is much simpler and is used in further discussion. The general idea of the deduction is based on a relationship between the symmetry operations and the symbolic formula. The symmetry operations present in the chain or in a pair of chains remain in the structure only when all other chains are consistent with them. This

Table 6. *Combinatorial deduction of the SPT layer symmetry*

α and pairs – also includes cases when the formula is divided into symmetric parts by a pair of symbols $\alpha\alpha$, $\beta\beta$, $\gamma\gamma$ or $\delta\delta$.

Symmetric partition of the symbol by				$\Sigma(\beta,\delta)$ and $\Sigma(\gamma,\delta)$				
α and pairs 2_1 (y)	β -1	γ b (z)	δ 2 (x)	$2n+1, 2n$ c (y)	$2n, 2n+1$ c (x)	$2n+1, 2n+1$ 2_1 (z)	Layer symmetry	Simplest formula
+	+	−	−	(+)	−	−	$p12_1/c$	$\beta\beta$, $\beta'\beta'$
	−	+	−	−	(+)	−	$pc2_1b$	$\gamma\gamma$
		−	+	−	−	(+)	$p22_12_1$	$\delta\delta$
			−	−	−	−	$p12_11$	α, α'
−	+	+	−	−	−	(+)	$p112_1/b$	$\beta\gamma\beta\gamma$
		−	+	−	(+)	−	$p2/c11$	$\beta\delta\beta\delta$
			−	−	−	−	$p\bar{1}$	$\beta\delta\gamma\beta\gamma\delta$, $\beta\beta'$
	−	+	+	(+)	−	−	$p2cb$	$\delta\gamma\delta\gamma$
			−	−	−	−	$p11b$	$\gamma\delta\beta\gamma\beta\delta$
		−	+	−	−	−	$p211$	$\delta\gamma\beta\delta\beta\gamma$
			−	+	−	−	$p1c1$	$\alpha\gamma\delta\alpha\gamma\delta$
				−	+	−	$pc11$	$\alpha\beta\delta\alpha\beta\gamma$
					−	+	$p112_1$	$\alpha\beta\gamma\alpha\beta\gamma$
						−	$p1$	$\beta\delta\gamma$

consistency is reflected in the formula. For example, the chain symmetry, 2_1 screw axis, remains in the layer when the formula is divided into symmetric parts with pairs of symbols, *e.g.* $\alpha\alpha$, $\beta\beta$, *etc*. This axis transforms the chain into itself. The same symmetry operation also appears when the symbolic formula is divided into symmetric parts with a single α symbol, but in this case the screw axis transforms adjacent chains into each other. The other types of chain linking, β, γ and δ, yield a symmetry center between the chains, a b glide plane parallel to the z axis and a twofold rotation axis along the x axis, respectively. This is reflected in the first four columns in Table 6, where '+' and '−' show the presence or absence of the conforming partitions of the formula, respectively. The conforming symmetry operations are provided in the third row of the table. Because of the chain inversion, the odd sum of β and δ symbols or γ and δ in the layer symbol requires a doubled formula (underlined in Table 6) to make it consistent with the repeat unit of the structure. These relations additionally yield three symmetry operations that are shown in Table 6 in the columns headed $\Sigma(\beta,\delta)$ and $\Sigma(\gamma,\delta)$. Finally, the symmetry of the layers and simplest relative symbolic formulae are shown in the last two columns.

Thus, this deduction results in ten possible symmetry groups for the V_6O_{14} layers. The known layer types (α, β and γ) represent the simplest formula for three of the four high-symmetry cases (the first four rows in Table 6). In this case, the symmetry operations for each chain (2_1 axis) as well as symmetry operations for the pair of chains, are crystallographic and, therefore, only the one symmetrically independent chain is present. More complicated layers probably could exist in the presence of a few different interlayer species.

While this manuscript was under review, a new member of the V_6O_{14} series was reported by Wang *et al.* (1999): $(tma)_2[Co(H_2O)_4]V_{12}O_{28}$. This structure has two types of links between the chains β and β', probably due to the two types of intercalated ions tma^+ and $[Co(H_2O)4]^{2+}$. In this structure, as well as in all simple V_6O_{14} structures (Table 5), only one symmetrically independent chain is present; however, in this case the chain symmetry is lowered to $\wp1$ from $\wp2_1$.

The work at Binghamton was supported by the National Science Foundation through grant DMR-9810198. We also thank Professor Jon Zubieta and Dr Dave Ross from Syracuse University, NY, USA, for the use of the single-crystal diffractometer.

References

Akselrud, L. G., Zavalij, P. Y., Grin, Yu. N., Pecharsky, V. K. & Fundamenskii, V. S. (1989). *12th European Crystallogr. Metting, Collected Abstracts, Moskow*; *Z. Kristallogr.* **3**(Suppl. 2), 155–155.

Biosym Technologies Inc. (1995). *Insight II. User's Guide.* October 1995., San Diego: Biosym/MSI.

Chen, R., Zavalij, P. Y. & Whittingham, M. S. (1999). *J. Mater. Chem.* pp. 93–100.

Chirayil, T. G., Boylan, E. A., Mamak, M., Zavalij, P. Y. & Whittingham, M. S. (1997). *Chem. Commun.* pp. 33–34.

Chirayil, T., Zavalij, P. Y. & Whittingham, M. S. (1996*a*). *J. Electrochem. Soc.* **143**, L193–L195.

Chirayil, T., Zavalij, P. Y. & Whittingham, M. S. (1996*b*). *Solid State Ion.* **84**, 163–168.

Chirayil, T., Zavalij, P. Y. & Whittingham, M. S. (1997). *J. Mater. Chem.* pp. 2193–2197.

Chirayil, T., Zavalij, P. Y. & Whittingham, M. S. (1998). *Acta Cryst.* C**54**, 1441–1444.

Crystal Structure Design (1997). *CrystalDesigner User's Guide.* Crystal Structure Design AS, Norway.

Dornberger-Schiff, K. (1966). *Lehrgang über OD-Strukturen*. Berlin: Akademie-Verlag.

Evans, H. T. Jr & Brusewitz, A. M. (1994). *Acta Chem. Scand.* **48**, 533–536.

Galy, J. & Carpy, A. (1975). *Acta Cryst.* B**31**, 1794–1795.

Farrugia, L. J. (1997). *J. Appl. Cryst.* **29**, 565.
Janauer, G. G., Dobley, A. D., Zavalij, P. Y. & Whittingham, M. S. (1997). *Chem. Mater.* **9**, 647–649.
Mazhar-Ul-Haque, Caugglan, C. N. & Emerson K. (1970). *Inorg. Chem.* **9**, 2421–2424.
Nazar, L. F., Koene, B. E. & Britten, J. F. (1996). *Chem. Mater.* **8**, 327–329.
Pecquenard, B., Zavalij, P. Y. & Whittingham, M. S. (1998*a*). *J. Mater. Chem.* pp. 1255–1258.
Pecquenard, B., Zavalij, P. Y. & Whittingham, M. S. (1998*b*). *Acta Cryst.* C**54**, 1833–1835.
Riou, D. & Férey, G. (1995*a*). *J. Solid State Chem.* **120**, 137–145.
Riou, D. & Férey, G. (1995*b*). *Inorg. Chem.* **34**, 6520–6523.
Sheldrick, G. M. (1996). *SADABS. Empirical Absorption Correction Program.* University of Göttingen, Germany.
Siemens (1995). *SMART and SAINT. Data Collection and Processing Software for the SMART System.* Siemens Analytical X-ray Instruments Inc., Madison, Wisconsin, USA.
Walk, C. R. & Gore, J. S. (1975). *J. Electrochem. Soc.* **122**, 68C.
Waltersson, K. & Forslund, B. (1977*a*). *Acta Cryst.* B**33**, 784–789.
Waltersson, K. & Forslund, B. (1977*b*). *Acta Cryst.* B**33**, 789–793.
Wang, X., Lin, L., Jacobsen, A. J. & Ross, K. (1999). *J. Mater. Chem.* **9**, 859–861.
Weeks, C., Zavalij, P. Y. & Whittingham, M. S. (1999). *Inorg. Chem.* In the press.
Whittingham, M. S. (1976). *J. Electrochem. Soc.* **123**, 315–320.
Whittingham, M. S., Chen, R., Chirayil, T. & Zavalij, P. Y. (1996). *Electrochem. Soc. Proc.* **96–95**, 76–85.
Zavalij, P. Y., Chirayil, T. & Whittingham, M. S. (1997*a*). *Acta Cryst.* C**53**, 879–881.
Zavalij, P. Y., Chirayil, T. & Whittingham, M. S. (1997*b*). *Z. Kristallogr.* **212**, 321–322.
Zavalij, P., Whittingham, M. S., Boylan, E. A., Pecharsky, V. K. A. & Jacobson, R. A. (1996). *Z. Kristallogr.* **211**, 464.
Zavalij, P. Y., Whittingham, M. S., Chirayil, T., Pecharsky, V. K. & Jacobson, R. A. (1997). *Acta Cryst.* C**53**, 170–171.
Zavalij, P. Y., Zhang, F. & Whittingham, M. S. (1997). *Acta Cryst.* C**53**, 1738–1739.
Zhang, Y., DeBord, J. R. D., O'Connor, C. J., Haushalter, R. C., Clearfield, A. & Zubieta, J. (1996). *Angew. Chem. Int. Ed. Engl.* **35**, 989–991.
Zhang, Y., Haushalter, R. C. & Clearfield, A. (1996). *Chem. Commun.* pp. 1055–1056.
Zhang, F., Zavalij, P. Y. & Whittingham, M. S. (1998). *Mater. Res. Soc. Proc.* **496**, 367–372.